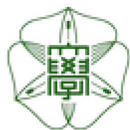
HOKKAIDO UNIVERSITY

Title	Experimental and numerical study on phase change material (PCM) for thermal management of mobile devices
Author(s)	Tomizawa, Yusuke; Sasaki, Katsuhiko; Kuroda, Akiyoshi; Takeda, Ryo; Kaito, Yoshihiko
Citation	Applied Thermal Engineering, 98, 320-329 https://doi.org/10.1016/j.applthermaleng.2015.12.056
Issue Date	2016-04-05
Doc URL	http://hdl.handle.net/2115/68706
Rights	© 2016. This manuscript version is made available under the CC-BY-NC-ND 4.0 license http://creativecommons.org/licenses/by-nc-nd/4.0/
Rights(URL)	http://creativecommons.org/licenses/by-nc-nd/4.0/
Type	article (author version)
File Information	Manuscript.pdf

Instructions for use

Hokkaido University Collection of Scholarly and Academic Papers : HUSCAP

Experimental and Numerical Study on Phase Change Material (PCM) for Thermal Management of Mobile Devices

Yusuke TOMIZAWA[*1], Katsuhiko SASAKI[*2], Akiyoshi KURODA[*2], Ryo TAKEDA[*2] and Yoshihiko KAITO[*3]

[*1] Graduate School of Engineering, Hokkaido University, Kita 13, Nishi 8, Kita-ku, Sapporo, Hokkaido 060-8628, Japan

[*2] Faculty of Engineering, Hokkaido University, Kita 13, Nishi 8, Kita-ku, Sapporo, Hokkaido 060-8628, Japan

[*3] Fujitsu Limited, Kita 7, Nishi 4-3-1, Kita-ku, Sapporo, Hokkaido 060-0807, Japan

*Corresponding Author:

Katsuhiko SASAKI, Ph.D
Professor, Faculty of Engineering, Hokkaido University
Kita 13, Nishi 8, Kita-ku, Sapporo, Hokkaido 060-8628, Japan
Tel/Fax: +81-011-706-8376, E-mail:katsu@eng.hokudai.ac.jp

Keywords: Phase Change Material (PCM), Thermal management, Passive cooling, Mobile device, Finite element method (FEM)

***Word count*:** 4060 words (Introduction through Conclusion)

***Manuscript Type*:** Research Paper

Abstract

As mobile devices become more complex and higher in performance despite the smaller in size, heat concentration at localized areas has become a problem. In recent years, passive cooling using phase change materials (PCMs) have drawn attention as thermal management methods for mobile devices. PCMs reduce the temperature increase rate due to their latent heat properties. This reduction in the temperature increase rate is called a “delay effect”. Moreover, microencapsulated PCMs (MPCMs) are attracting attention because they keep the melted PCMs from leaking. In this study, PCM sheets containing MPCM/polyethylene composite material are investigated for the thermal management of mobile devices. Namely the authors conduct a series of experiments using the PCM sheet with high thermal conductivity sheet mounted into a simply modeled mobile device. Effects of the mass, the latent heat, the thermal conductivity, the configuration of the PCM sheet, and high thermal conductivity sheet on the temperature of a smart phone simulator are investigated. A finite element analysis (FEA) is also conducted considering the phase change of PCMs to investigate the optimal dimension and shape of PCMs. As a result, the delay effect of PCMs and effectivity of a copper sheet pasted on the PCMs are verified by experiments. Moreover, FEA shows that using the PCM sheet with high thermal conductivity sheet has an advantage for the thermal management of mobile devices and gives an optimal condition of the PCM sheets.

46 ## 1. Introduction

47 In recent years, complex and high-performance mobile electronic devices such as smart phones
48 and tablet PCs have been spreading widely. However, the power density of these devices has become
49 higher and the heat dissipation area smaller [1]. This will eventually lead to overheating and damage
50 the components on the substrate due to the acceleration of the thermal fatigue in the solder [2]. In
51 addition, high surface temperature of the mobile devices will lead to discomfort during usage [3].
52 Thus, thermal management of mobile devices is quite important.

53 Active thermal management using fans is a popular method for cooling electronic devices [4].
54 However, mobile electronic devices do not have enough space to insert fans or heat sinks [5]. In
55 addition, fans are inadequate for use with mobile devices due to noise, maintenance, and additional
56 power consumption [6]. Therefore passive thermal management is widely chosen as the cooling
57 method of mobile devices. Phase change materials (PCMs) have attracted a lot of attention for high
58 efficient passive cooling functions of mobile devices. As PCMs absorb heat at a constant temperature
59 due to their latent heat during melting process, the temperature increase rate of PCMs decreases,
60 which is called a "delay effect" in this paper. This suggests that there is a possibility of controlling
61 the surface temperature of the mobile devices by using PCMs.

62 The thermal management of electronic devices using PCMs has been studied by many researchers.
63 For example, Alawadhi and Amon conducted experimental and numerical studies on PCM thermal
64 control unit (TCU) for portable electronic devices and showed the effects of the power operation and
65 the Stefan number [7]. Tan *et al.* carried out a series of experiments using heat storage unit (HSU)
66 and heat sink filled with PCM and clarified the effect of heat distribution [8], number of fins in the
67 heat sink [1,6], the power levels [6], and steady and transient state heating conditions [1]. Numerical
68 simulations were also performed to study the effects of power levels, number of fins, fin height, and
69 fin thickness [9]. Ishizuka *et al.* conducted numerical simulation of electronic devices including
70 PCM with thermal network method [10-12]. Kandasamy *et al.* carried out experiments of PCM
71 package for thermal management of portable electronic devices to investigate the effect of power
72 input, orientation of package, and various melting/freezing times [13]. They also conducted both
73 experimental and numerical investigation of PCM-based heat sink for thermal management of

74 transient electronic devices to reveal the effects of power level and designs of heat sinks [14].
75 Mahmoud *et al.* experimentally investigated the effects of heat sink configuration, power level, and
76 PCM type for PCM based heat sinks [15]. Qu *et al.* studied the heat sink with copper metal foam–
77 paraffin composite [16]. Passive cooling system using PCM for high-powered Li-ion battery package
78 was investigated by Kizilel *et al.* [17] and Li *et al.* [18]. As shown above, almost all studies focused
79 on relatively large size devices such as heat sinks and Li-ion battery packages, and there are few
80 research works to verify the applicability of PCMs to mobile devices.

81 In order to apply PCMs to mobile devices, it is necessary to seal PCMs to prevent melted PCMs
82 from leaking. Recently, studies on microencapsulated PCMs (MPCMs), in particular, MPCM
83 composite materials have been carried out. The advantages of MPCMs are preventing the liquid
84 PCM leakage and adapting various materials for heat storage by compounding MPCMs into various
85 materials. Yoshinori *et al.* measured thermophysical properties of composite materials containing
86 silicon rubber and MPCMs [19]. Katsuragi *et al.* conducted experiments under unsteady heat
87 conduction and also verified the effect of the composites by a numerical simulation model [20].
88 Wang *et al.* fabricated phase change composites containing MPCMs, expanded graphite, and high
89 density polyethylene. They clarified the thermal conductivity enhancement of the composites [21].
90 Zhang *et al.* investigated the melting thermal performances of MPCM composite plate containing
91 carbon fibers, aluminum powder, and silica aerogel [22]. The physical properties of the MPCM
92 composites have been also studied by some researchers [23-29]. However, the understanding of
93 thermophysical properties of MPCM composites is not sufficient. This means that it is difficult to
94 obtain optimal conditions for thermal control using PCMs by numerical simulation.

95 In this study, the authors fabricate an experimental system simulating a mobile smart phone. The
96 system contains substrate, heater, case, and sheets made of MPCM/polyethylene composite. Both
97 experimental and numerical investigations are conducted to verify the applicability of PCMs to the
98 thermal management of mobile devices. First, experiments to clarify the mass effect of PCM sheet on
99 the temperature change are carried out using the experimental system. Afterwards, experiments to
100 investigate the effects of latent heat, thermal conductivity, and configuration of the PCM sheets on
101 the temperature change are also carried out. Moreover, a copper sheet, as a high thermal conductivity

102 material, is incorporated in the experimental system and the effect of a copper sheet on the phase
103 change of the PCM sheet is revealed. Finally, numerical simulations to estimate the thermophysical
104 properties of the MPCM/polyethylene composite are conducted using finite element method (FEM).
105

106 2. Experiment on Thermal Characteristic of PCM Sheets

107 2.1 Experimental method

108 2.1.1 PCM sheet

109 Paraffin is used as the PCM in this study. Paraffin has higher latent heat than other PCMs such as
110 organic salt and inorganic salt. The PCM is microencapsulated by melamine resin to prevent the
111 melted paraffin from leaking. The MPCM can be applied to the mobile devices such as smart phones
112 because of its leak-proof characteristic. PMCD-32SP (Miki Riken Industrial Co., Ltd.) is chosen as
113 the MPCM for this study. The physical properties of the MPCM are shown in Table 1. As shown in
114 Fig. 1(a), since the MPCM is in powder form, the MPCM is ordinary used as master batches made by
115 combining 50wt% polyethylene and 50wt% MPCM, shown in Fig. 1(b).
116 Figure 2 shows a metal mold used to make the PCM sheets. First, the mold is put on a hot plate
117 and heated up to 150°C. After that, the MPCM master batch is put into the mold and a stainless steel
118 plate is set on the master batch with 40 N load. Finally the PCM sheet can be obtain after cooling the
119 mold. In this procedure, three different types of the mass of PCM sheets are prepared. Figure 3
120 shows a photo of the PCM sheet. The size and mass of the PCM sheets are shown in Table 2.
121

122 2.1.2 Experimental procedure

123 Figure 4 shows the main test part in this experiment. The case in Fig. 4 is made of 1 mm thick
124 polycarbonate boards and the size of the case is 122 mm length, 62 mm width, and 11 mm height,
125 respectively. The PCM sheet is put on a rubber heater and they are also put on a heat insulator
126 covered by the case. T-type thermocouples are used to measure the temperature. Three
127 thermocouples are attached to the heater, the PCM sheet, and the case as shown in Fig. 4(b). The
128 thermocouples for the PCM sheet and the case are inserted into small grooves with epoxy resin to fill
129 the clearance. Kapton tape is then used to fix the thermocouples firmly. No special grooves are

130 prepared on the surface of the heater and only kapton tape is used to attach the thermocouple. An
131 additional thermocouple is used to measure the ambient temperature. The thermocouples used were
132 calibrated within the range of 0-100°C and have an uncertainty of 0.5°C.

133 A power supply is used to give accurate power of 2.00 W to the heater. The temperatures at each
134 point are measured just after heating starts. The measurements of the temperatures are conducted
135 every minute during 90 minutes of heating. The experiment is conducted three times under the same
136 experimental condition. Four experimental conditions are chosen; no PCM sheet, PCM sheet A (5.10
137 g), PCM sheet B (7.22 g), and PCM sheet C (9.86 g).

138

139 2.1.3 Experimental data processing

140 In order to remove the influence of the ambient temperature variation, a value of temperature rise
141 is used as the value to evaluate the thermal characteristic of the PCM sheet. The temperature rise is
142 defined as the difference between the measured temperature and the ambient temperature. In addition,
143 values of maximum temperature rise and saturation time are used for the evaluation. The value of
144 saturation time means the time until the temperature becomes a constant value.

145 To determine the maximum temperature and the saturation time, noise of the measurement is
146 reduced as follows. The following fitting function of $\Delta T_f(t)$ is used,

147 $$\Delta T_f(t) = A_1 \,\mathrm{erf}(B_1 t) + A_2 \,\mathrm{erf}(B_2 t) + A_3 \,\mathrm{erf}(B_3 t) + C \tag{1}$$

148 $$\mathrm{erf}(t) = \frac{2}{\sqrt{\pi}} \int_0^t e^{-\tau^2} \mathrm{d}\tau \tag{2}$$

149 where A_1, A_2, A_3, B_1, B_2, B_3 and C are fitting constants, and erf(t) is Gauss error function. Figure 5(a)
150 shows an example of fitting curve of the case temperature without PCM sheet, and Fig. 5(b) with
151 PCM sheet C (9.86 g). Figure 5 also shows the definitions of both the maximum temperature rise
152 ΔT_{max} and the saturation time t_{sat}. These values are obtained by using the fitting curves.

153

154 2.2 Experimental results and discussion

155 Figure 6 shows the relationship between the value of temperature rise and time of no PCM sheet,

156 PCM sheet A (5.10 g), B (7.22 g) and C (9.86 g). Figure 6(a) shows the heater temperature and Fig.
157 6(b) the case temperature. The PCM sheet affects the temperature variation: the inflection parts of
158 the temperature rise variation can be seen as shown in Fig. 6 by a circle. While the PCM is melting,
159 the polyethylene composing the PCM sheet conducts heat. Therefore, the period in which the
160 temperature remains relatively constant does not appear. However, decrease in the temperature
161 increasing rate is shown clearly, which indicates the effect of the PCM. Moreover, the temperature
162 rise rates with the PCM sheet are slower than that without the PCM sheet. Namely, the PCM sheets
163 lead to the delay effect due to their latent heat.

164 The PCM sheets increase the temperature rise of the heater as shown in Fig. 6(a). On the other
165 hand, the PCM sheets decrease the temperature rise of the case as shown in Fig. 6(b). The reason of
166 the countertrend between the temperatures of the heater and the case is because the thermal
167 resistance between the heater and the case with the PCM sheet is larger than that without the PCM
168 sheet. That is, the PCM sheet suppresses the generation of natural convection and the heat transfer in
169 the inner air.

170 As for the effect of the mass of the PCM sheet on temperature, the mass of the PCM sheet affects
171 temperature as shown in Fig. 6. The temperature rise of the heater becomes lower with increase in
172 the mass of the PCM sheets. As shown in Table 2, the thickness of the PCM sheets increases and the
173 thickness of the layer of the inner air decreases with increase in the mass of the PCM sheets. Most of
174 heat is transferred by thermal conduction in the inner air. Therefore, the overall thermal resistance
175 decreases with decrease in the thickness of the layer of the inner air and with increase in the
176 thickness of the PCM sheets.

177 Figure 7 shows the relationship between the mass of the PCM sheets and the saturation time. The
178 symbols show the average of three times of experiment. The saturation time increases with increase
179 in the mass of the PCM sheets as shown in Fig. 7. The larger delay effect can be seen with increase
180 in the mass of the PCM sheets. A linear relationship between the mass of the PCM sheets and the
181 saturation time can be also seen in Fig.7.

182

183 3. Experiment on Application of PCM Sheets to Smart Phone Simulator

184 3.1 Experimental procedures

185 3.1.1 Preparation of modified PCM sheets and a PE sheet

186 Considering actual used conditions of mobile phones, a small mold is used to modify the PCM
187 sheets for the conditions. To clarify the effect of the latent heat of the PCM sheet, a polyethylene
188 sheet (PE sheet) is also made and compared with the PCM sheets. The polyethylene powder
189 (SUNFINE^{TM} XLH451) is used for the PE sheet. Figure 8 shows the equipment to mold the PCM and
190 the PE sheet. The steel mold serves as the punch guide to provide uniform thickness to the sheets.
191 The strong magnet is used to prevent leakage of the melted PCM master batch or PE powder from
192 the space between the mold and the aluminum plate. The PCM master batch or the PE powder is set
193 into the mold, and pressured by a punch in an electric furnace set at 155°C. Two PCM sheets in
194 different size of 25 × 25 × 4 mm and 50 × 50 × 1 mm, and a PE sheet of 25 × 25 × 4 mm are made
195 for the experiments. The PCM sheets of 25 × 25 × 4 mm and 50 × 50 × 1 mm have the same volume.
196 Figure 9 shows photos of the PCM sheets of 25 × 25 × 4 mm and 50 × 50 × 1 mm. PCM sheets lined
197 with copper sheets are prepared to clarify the advantage to use PCM sheets with high thermal
198 conductivity materials for mobile phones.

199

200 3.1.2 Experimental setup

201 Figure 10 shows a schematic diagram of the test section in the experiment. The front case is made
202 of polycarbonate boards and the rear case of acrylic board. A ceramic heater for simulating LSI is
203 fixed on a substrate by a double-sided thermal tape. A PCM (PE) sheet is also fixed on the heater by
204 the thermal tape. When the PCM sheets lined with copper sheets are used, the copper sheets are
205 attached to the heater. Namely, the copper sheet is situated between the heater and the PCM sheet.
206 Nine thermocouples are attached to the heater, the PCM (PE) sheet, the substrate, the front case, and
207 the rear case as shown in Fig. 10(b). An additional thermocouple is used to measure ambient
208 temperature.

209 The voltage of 8.5 V is applied to the heater, and the temperatures are measured just after the
210 heating starts. The power of the heater becomes 1.3 W in steady state. Temperatures are measured for
211 60 minutes during heating. Experiments are conducted three times with the same condition.

212

213 3.2 Experimental results and discussion

214 Figure 11 shows the relationship between the value of the temperature rise and time. Solid circles,
215 solid diamonds, solid triangles, solid squares, open triangles, and open squares show the results of no
216 sheet, PE sheet (25 × 25 × 4 mm), PCM sheet (25 × 25 × 4 mm), PCM sheet (50 × 50 × 1 mm), PCM
217 sheet (25 × 25 × 4 mm) lined with copper sheet, and PCM sheet (50 × 50 × 1 mm) lined with copper
218 sheet, respectively. Figure 11(a) shows the heater temperature and Fig. 11(b) the case temperature.
219 Figures 12 and 13 show the maximum temperature rise and the saturation time in all test conditions,
220 respectively. The temperature rise rate of the thick PCM sheet (25 × 25 × 4 mm) is slower than that
221 of the thin PCM sheet (50 × 50 × 1 mm) in spite of the same mass as shown in Fig. 11. Furthermore,
222 the temperature rise rate of the PCM sheets lined with copper sheets is slower than that of the PCM
223 sheets without copper sheets.

224 Focusing on the results of no sheet, PE sheet (25 × 25 × 4 mm), and PCM sheet (25 × 25 × 4 mm)
225 to clarify the effects of latent heat and thermal conductivity of the PCM in Fig. 12, the temperature
226 rise of the heater decreases by using the PCM (PE) sheet. Since the thermal conductivity of the PCM
227 sheet is higher than that of the PE sheet, the PCM sheet leads to higher temperature rise of the heater
228 than the PE sheet. Therefore, when replacing the inner air of the mobile devices with the PCM sheet,
229 the temperature of the LSI decreases. However, when replacing the resin components of the mobile
230 devices with the PCM sheet, the temperature of the LSI increases. As for the saturation time shown
231 in Fig. 13, the PCM sheet gives longer saturation time than the PE sheet. The PCM used in this study
232 has the same heat capacity as polyethylene. Therefore, the latent heat of the PCM has a larger effect
233 on the saturation time than the sensible heat.

234 The size effect of the PCM sheet on temperature is discussed comparing the results of two PCM
235 sheets of the same volume (same latent heat) but different size (25 × 25 × 4 mm and 50 × 50 × 1 mm).
236 The saturation time of the thick PCM sheet (25 × 25 × 4 mm) is longer than that of the thin PCM
237 sheet (50 × 50 × 1 mm) as shown in Fig. 13. Thus, the thickness of the PCM sheet has a large effect
238 on the saturation time. Therefore, when applying the PCM sheets in mobile devices, thicker PCM
239 sheets are more effective for the thermal design of mobile devices.

240 To discuss the effect of copper sheet on the temperature, the comparison between the results of
241 two PCM sheets (25 × 25 × 4 mm and 50 × 50 × 1 mm) lined with copper sheet is conducted. The
242 copper sheet decreases the temperature rise of the heater as shown in Fig. 12. By using the copper
243 foil, the temperature rise of the front case increases when the thick PCM sheet (25 × 25 × 4 mm) is
244 used, and decreases when the thin PCM sheet (50 × 50 × 1 mm) is used. This means that the uniform
245 temperature of the PCM sheet caused by the copper sheet leads to the large effect of the PCM on the
246 temperature rise. As for the saturation time, the thick PCM sheet gives longer saturation time as
247 shown in Fig. 13. Therefore, the PCM sheet lined with high thermal conductivity materials such as
248 copper sheet has an advantage in use with the mobile phones.

249

250
4. Numerical Simulation

251
4.1 FE model

252 In this study, the thermal fluid analysis considering the phase change of PCM is performed by
253 using ANSYS Fluent in commercial FEM analysis software ANSYS 14.5 (ANSYS, Inc.). Figure 14
254 shows a finite element (FE) model including a front case, a rear case, a substrate, a PCM (PE) sheet,
255 inner air, and nuts and bolts to fix the substrate. Total number of nodes and elements is 93196 and
256 317388, respectively. The FE model is made to reproduce the experimental setup.

257 The enthalpy-porosity method is used to express the phase change of the PCM sheets. The
258 enthalpy of the PCM sheet is represented by the sum of the sensible enthalpy and the latent enthalpy.
259 The latent enthalpy ΔH is provided by following equation,

260 $$\Delta H = \beta L \qquad (3)$$

261 where β and L is the liquid fraction and the latent heat of the material, respectively. The liquid
262 fraction β is equal to zero when the temperature is below the solidus temperature as the melting start
263 temperature. The liquid fraction β is equal to one when the temperature is above the liquidus
264 temperature as the melting finish temperature. The liquid fraction β is assumed to vary linearly in the
265 temperature range of the solidus temperature to the liquidus temperature. Additionally, the surface-
266 to-surface radiation model is used in order to express the radiation in the cases. The physical

267 properties used in this simulation are shown in Table 3. The physical properties of the PCM sheet are
268 estimated by simple mixing rules shown in (4)-(6) and the Bruggeman equation shown in (7).

269 $$\rho = \rho_1 \phi_1 + \rho_2 \phi_2 \quad (4)$$

270 $$c_p = \frac{\rho_1 c_{p1} \phi_1 + \rho_2 c_{p2} \phi_2}{\rho} \quad (5)$$

271 $$L = \frac{\rho_1 L_1 \phi_1 + \rho_2 L_2 \phi_2}{\rho} \quad (6)$$

272 $$1 - \phi = \left(\frac{k_p - k_c}{k_p - k_m} \right) \left(\frac{k_m}{k_c} \right)^{1/3} \quad (7)$$

273 where ρ, c_p, k and ϕ are the density, the specific heat, the thermal conductivity, and the volume
274 fraction, respectively. The subscript numbers of 1 and 2 in (4)-(6) mean the material type. The
275 subscript *m*, *p*, and *c* in (7) mean the matrix, the particle, and the compound, respectively. The
276 physical properties of the PCM sheet are shown in Table 4. In addition, the viscosity of the PCM
277 sheet is required because the phase change materials have to be treated as a fluid. In this simulation,
278 the viscosity of the PCM sheet is provided with the value of 1 Pa·s. The value of 1 Pa·s was selected
279 from the viewpoint of both calculation precision and calculation time.
280
281 4.2 Numerical conditions
282 The FE analysis is conducted for 60 minutes just after heating starts. The power of the heater is
283 given the same value of 1.3 W as the experiment. The thermal contact resistances between the heater
284 and the substrate, and between the heater and the PCM (PE) sheet are set to 15×10^{-4} $m^2 \cdot K/W$. The
285 value is obtained by optimizing the temperature of each part comparing the simulation with
286 experiments. The contact resistances include the thermal resistance of the thermal tape. The initial
287 condition of the temperature is set to 19°C. The ambient temperature is also the constant value of
288 19°C. The heat transfer coefficients on the upper surface, the side surface, and the bottom surface of
289 the cases are provided with 5.7 $W/m^2 \cdot K$, 6.0 $W/m^2 \cdot K$, and 3.7 $W/m^2 \cdot K$, respectively. The values were
290 based on empirical laws of natural convection [30]. The emissivity of the surface of the cases is also

291 provided with 0.9 to express the heat dissipation from the surface of the case by both the convection
292 and the radiation. The pressure-based coupled algorithm of ANSYS Fluent is selected to use the
293 pressure-velocity coupling.
294

295 4.3 Numerical results and discussion

296 Figure 15 shows the comparison between the results of the solid model and the phase change
297 model using the PE sheet. The solid, broken, and dot dash lines show the temperature rise variation
298 of the heater, the PE sheet, and the front case, respectively. The difference between the results of the
299 solid model and the phase change model are within 0.4°C. Therefore, reasonable numerical results
300 can be obtained by considering the PCM sheet as the fluid material having the viscosity of 1 Pa·s.
301 Figure 16 shows the comparison between the numerical and the experimental results of no sheet,
302 PE sheet, PCM sheet of 25×25×4 mm, and PCM sheet of 50×50×1 mm, respectively. In Fig. 16, solid
303 and broken lines show numerical results of the heater and the front case, while diamonds and squares
304 show the experimental results of the heater and the front case, respectively. The numerical results
305 have good agreements with the experimental results as shown in Fig. 16. These results suggest that
306 the physical properties of the MPCM/polyethylene composite can be estimated by using the mixing
307 rules and Bruggeman equation. Therefore, optimal thermal design to apply the PCM sheets to the
308 mobile phones may be easily conducted using the material properties obtained in the same way.
309

310 5. Conclusion

311 The aim of this paper was to investigate the application of PCM sheets to mobile phones. The
312 thermal behavior of the PCM sheets was clarified using the smart phone simulator. The numerical
313 simulations considering the phase change of the PCM sheet were also conducted by FE analysis. As a
314 result, the following conclusions were obtained:

315 (1) The PCM sheets leads to the delay effect. Namely, the saturation time increases with increase in
316 the mass of the PCM sheet, and there is a linear relationship between the mass of the PCM sheet
317 and the saturation time.

318 (2) The latent heat of the PCM has a larger effect on the saturation time than the sensible heat.

319 (3) Since the thermal conductivity of the PCM sheet is higher than that of the PE sheet, the PCM
320 sheet leads to higher temperature rise of the heater than the PE sheet, and also leads to lower
321 temperature rise of the surface of the case than the PE sheet.

322 (4) The thickness of the PCM sheet has a large effect on the saturation time. Therefore, when
323 applying the PCM sheets to the mobile devices, thicker PCM sheets are more effective for the
324 thermal design.

325 (5) The copper sheet leads to low temperature rise and hardly affects the saturation time. Therefore,
326 thick PCM sheets should be used alongside high thermal conductivity sheets.

327 (6) The estimation of the thermophysical properties of the MPCM composite by the mixing rules
328 and Bruggeman equation can be adapted to simulate the heat transfer considering the phase
329 change. This suggests that an optimal thermal design to apply the PCM sheets to the mobile
330 phones may be easily conducted using the material properties obtained in the same way.

331

332 [Reference]

333 [1] G. Setoh, F.L. Tan, S.C. Fok, Experimental studies on the use of a phase change material for
334 cooling mobile phones, International Communications in Heat and Mass Transfer, Vol.37
335 (2010), pp.1403-1410

336 [2] Y. Nishino, M. Ishizuka, S. Nakagawa, Study on the Enhancement of Natural Air Cooling
337 Capability in the Vertical Channel Model of Compact Electronic Equipment (The Effect of the
338 Clearance of a Channel on the Natural Cooling Capability) (in Japanese), Transactions of the
339 Japan Society of Mechanical Engineers. B, Vol.75, No.755 (2009), pp.1479-1484

340 [3] Y. Shinki, S. Ubemoto, N. Kishimoto, D. Takeda, Y. Yamane, H. Miyoshi, The Thermal Design
341 for Mobile Phones by Using Thermal Simulation System (in Japanese), Proceedings of Thermal
342 Engineering Conference (2007), pp.219-220

343 [4] Z.Ling, Z.Zhang, G.Shi, X.Fang, L.Wang, X.Gao, Y.Fang, T.Xu, S.Wang, X.Liu, Review on
344 thermal management systems using phase change materials for electronic components, Li-ion
345 batteries and photovoltaic modules, Renewable and Sustainable Energy Reviews, Vol.31 (2014),
346 pp.427-438

347 [5] Z. Luo, H. Cho, X. Luo, K.-i. Cho, System thermal analysis for mobile phone, Applied Thermal
348 Engineering, Vol.28 (2008), pp.1889-1895

349 [6] S.C. Fok, W. Shen, F.L. Tan, Cooling of portable hand-held electronic devices using phase
350 change materials in finned heat sinks, International Journal of Thermal Sciences, Vol.49 (2010),
351 pp.109-117

352 [7] E.M. Alawadhi, C.H. Amon, PCM Thermal Control Unit for Portable Electronic Devices:
353 Experimental and Numerical Studies, IEEE Transactions on Components and Packaging
354 Technologies, Vol. 26 (2003), No. 1, pp.116-125

355 [8] F.L. Tan, C.P. Tso, Cooling of mobile electronic devices using phase change materials, Applied
356 Thermal Engineering, Vol.24 (2004), pp.159-169

357 [9] S.F. Hosseinizadeh, F.L. Tan, S.M. Moosania, Experimental and numerical studies on
358 performance of PCM-based heat sink with different configurations of internal fins, Applied
359 Thermal Engineering, Vol.31 (2011), pp.3827-3838

360 [10] N. Fujii, M. Ishizuka, S. Nakagawa, Application of a thermal network method to the thermal
361 analysis of electronic devices including phase change materials (in Japanese), In: Proceedings
362 of the 44th Conference of The Japan Society of Mechanical Engineers Hokuriku Shin-etsu
363 Branch (2007), pp.315-316
364 [11] N. Fujii, S. Takakuwa, M. Ishizuka, S. Nakagawa, Application of a thermal network method
365 to the thermal analysis of electronic devices including phase change materials (in Japanese), In:
366 Proceedings of the 45th Conference of The Japan Society of Mechanical Engineers Hokuriku
367 Shin-etsu Branch (2008), pp.245-246
368 [12] S. Takakuwa, M. Ishizuka, S. Nakagawa, Application of a Thermal Network Method to
369 Thermal Analysis of Electronic Device with Phase Change Materials: Modeling Technique of
370 Latent Heat (in Japanese), In: Proceedings of the 46th Conference of The Japan Society of
371 Mechanical Engineers Hokuriku Shin-etsu Branch (2009), pp.169-170
372 [13] R. Kandasamy, X.-Q. Wang, A.S. Mujumdar, Application of phase change materials in
373 thermal management of electronics, Applied Thermal Engineering, Vol.27 (2007), pp.2822-
374 2832
375 [14] R. Kandasamy, X.-Q. Wang, A.S. Mujumdar, Transient cooling of electronics using phase
376 change material (PCM)-based heat sinks, Applied Thermal Engineering, Vol.28 (2008),
377 pp.1047-1057
378 [15] S. Mahmoud, A. Tang, C. Toh, R. AL-Dadah, S.L. Soo, Experimental investigation of inserts
379 configurations and PCM type on the thermal performance of PCM based heat sinks, Applied
380 Energy, Vol.112 (2013), pp.1349-1356
381 [16] Z.G. Qu, W.Q. Li, J.L. Wang, W.Q. Tao, Passive thermal management using metal foam
382 saturated with phase change material in a heat sink, International Communications in Heat and
383 Mass Transfer, Vol.39 (2012), pp.1546-1549
384 [17] R. Kizilel, R. Sabbaha, J. R. Selmana, S. Al-Hallaj, An alternative cooling system to enhance
385 the safety of Li-ion battery packs, Journal of Power Sources, Vol.194 (2009), pp.1105-1112
386 [18] W.Q. Li, Z.G. Qu, Y.L. He, Y.B. Tao, Experimental study of a passive thermal management
387 system for high-powered lithium ion batteries using porous metal foam saturated with phase

388 change materials, Journal of Power Sources, Vol.255 (2014), pp.9-15
389 [19] K. Yoshinori, D. Katsuragi, J. Ogawa, H. Soeda, Unsteady Heat Conduction of Composite
390 Materials Using Micro Encapsulated Phase Change Materials (MEPCM) (in Japanese),
391 Proceedings of Thermal Engineering Conference 2007, pp.117-118
392 [20] D. Katsuragi, H. Soeda, Unsteady Heat Conduction of Composite Materials of Micro
393 Encapsulated Phase Change Materials (MEPCM): Comparison of Experiment and Numerical
394 Simulation (in Japanese), Symposium on Environmental Engineering (2009), pp.463-466
395 [21] X. Wang, Q. Guo, J. Wang, Y. Zhong, L. Wang, X. Wei, L. Liu, Thermal conductivity
396 enhancement of form-stable phase-change composites by milling of expanded graphite, micro-
397 capsules and polyethylene, Renewable Energy, Vol.60 (2013), pp.506-509
398 [22] J.J. Zhang, Z.G. Qu, Z.G. Jin, Experimental study on the thermal characteristics of a
399 microencapsulated phase-change composite plate, Energy, Vol.71 (2014), pp.94-103
400 [23] J. Su, L. Ren, L. Wang, Preparation and mechanical properties of thermal energy storage
401 microcapsules, Colloid and Polymer Science, Vol.284 (2005), pp.224-228
402 [24] J.-F. Su, L.-X. Wang, L. Ren, Z. Huang, Mechanical Properties and Thermal Stability of
403 Double-Shell Thermal-Energy-Storage Microcapsules, Journal of Applied Polymer Science,
404 Vol.103, pp.1295-1302
405 [25] J. Li, P. Xue, W. Ding, J. Han, G. Sun, Micro-encapsulated paraffin/high-density
406 polyethylene/wood flour composite as form-stable phase change material for thermal energy
407 storage, Solar Energy Materials & Solar Cells, Vol.93 (2009), pp.1761-1767
408 [26] J.-F. Su, S.-B. Wang, J.-W. Zhou, Z. Huang, Y.-H. Zhao, X.-Y. Yuan, Y.-Y. Zhang, J.-B. Kou,
409 Fabrication and interfacial morphologies of methanol–melamine–formaldehyde (MMF) shell
410 microPCMs/epoxy composites, Colloid and Polymer Science, Vol.289 (2011), pp.169-177
411 [27] J.-F. Su, X.-Y. Wang, Z. Huang, Y.-H. Zhao, X.-Y. Yuan, Thermal conductivity of
412 microPCMs-filled epoxy matrix composites, Colloid and Polymer Science, Vol.289 (2011),
413 pp.1535-1542
414 [28] S. Marchi, S. Pagliolico, G. Sassi, Characterization of panels containing micro-encapsulated
415 Phase Change Materials, Energy Conversion and Management, Vol. 74 (2013), pp.261-268

416 [29] M. Karkri, M. Lachheb, Z. Nógellová, B. Boh, B. Sumiga, M.A. AlMaadeed, A. Fethi, I.
417 Krupa, Thermal properties of phase-change materials based on high-density polyethylene filled
418 with micro-encapsulated paraffin wax for thermal energy storage, Energy and Buildings, Vol.88
419 (2015), pp.144-152
420 [30] The Japan Society of Mechanical Engineers ed., JSME Data Handbook: Heat Transfer 5th
421 Edition, The Japan Society of Mechanical Engineers, Tokyo, 2009, pp.52-53 (in Japanese)
422

423 **Figures Legends**

424 Fig. 1: Microencapsulated PCM and PCM master batch. (a) Microencapsulated PCM. (b) PCM
425 master batch.

426 Fig. 2: Aluminum mold and stainless steel plate.

427 Fig. 3: PCM sheet.

428 Fig. 4: Test section in experiment on thermal performance of PCM sheets. (a) General view. (b)
429 Cross-sectional view.

430 Fig. 5: Fitting curve and the definition of maximum temperature rise and saturation time. (a) Case
431 temperature without PCM sheet. (b) Case temperature when using PCM sheet C (9.86 g).

432 Fig. 6: Relationship between temperature rise and time. (a) Heater temperature. (b) Case
433 temperature.

434 Fig. 7: Relationship between mass of PCM master batch and saturation time.

435 Fig. 8: Manufacturing method of modified PCM sheet.

436 Fig. 9: Modified PCM sheet.

437 Fig. 10: Test section of the experiment on the application of the PCM sheet to the smart phone
438 simulator. (a) Dimensions. (b) Thermocouple locations. (c) Cross-sectional view.

439 Fig. 11: Relationship between temperature rise and time. (a) Heater temperature. (b) Front case
440 temperature.

441 Fig. 12: Maximum temperature rise at different conditions. (a) Heater temperature. (b) Front case
442 temperature.

443 Fig. 13: Saturation time at different conditions. (a) Heater temperature. (b) Front case temperature.

444 Fig. 14: Finite element model.

445 Fig. 15: Comparison between solid model and phase change model (L = 0 J/kg, μ = 1 Pa·s) with PE
446 sheet. (a) Solid model. (b) Phase change model (L = 0 J/kg, μ = 1 Pa·s).

447 Fig. 16: Comparison between numerical results and experimental results. (a) No sheet. (b) PE sheet
448 (25×25×4 mm). (c) PCM sheet (25×25×4 mm). (d) PCM sheet (50×50×1 mm).

449

450 **Tables Legends**

451 Table 1: Physical properties of microencapsulated PCM.

452 Table 2: Dimensions and mass of PCM sheets.

453 Table 3: Physical properties used in the simulation.

454 Table 4: Estimated physical properties of PCM sheet.

455

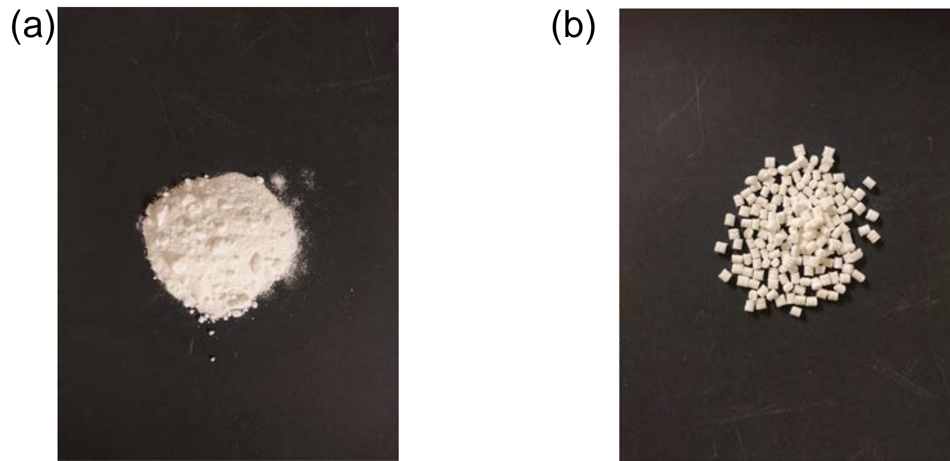

Fig. 1 Microencapsulated PCM and PCM master batch. (a) Microencapsulated PCM. (b) PCM master batch.

Fig. 2 Aluminum mold and stainless steel plate.

Fig. 3 PCM sheet.

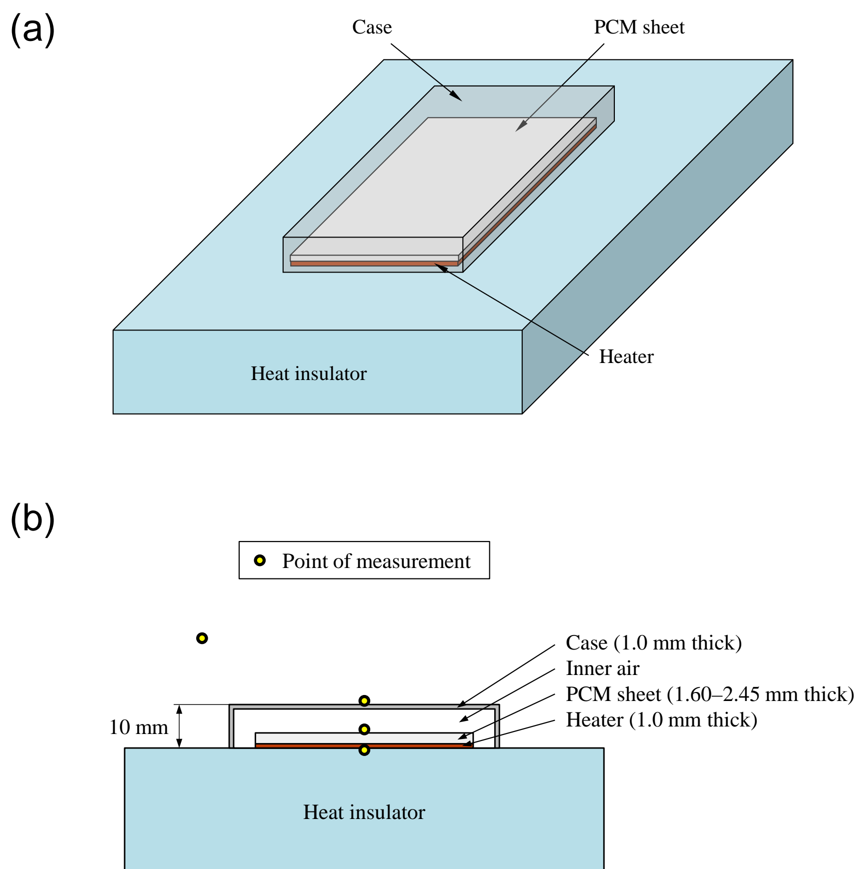

Fig. 4 Test section in experiment on thermal performance of PCM sheets. (a) General view. (b) Cross-sectional view.

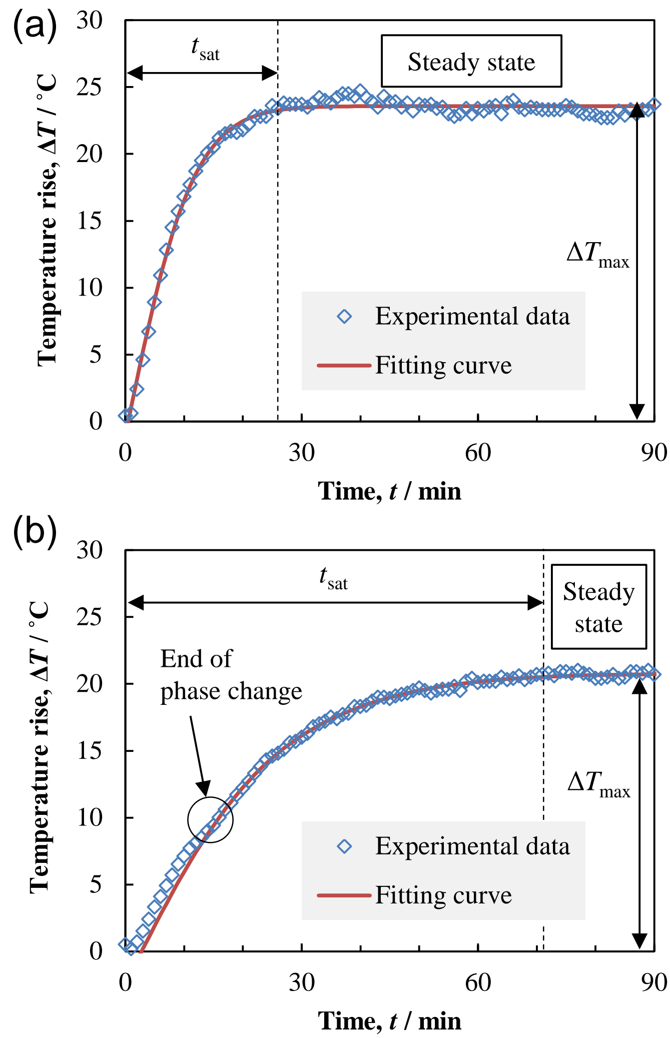

Fig. 5 Fitting curve and the definition of maximum temperature rise and saturation time. (a) Case temperature without PCM sheet. (b) Case temperature when using PCM sheet C (9.86 g).

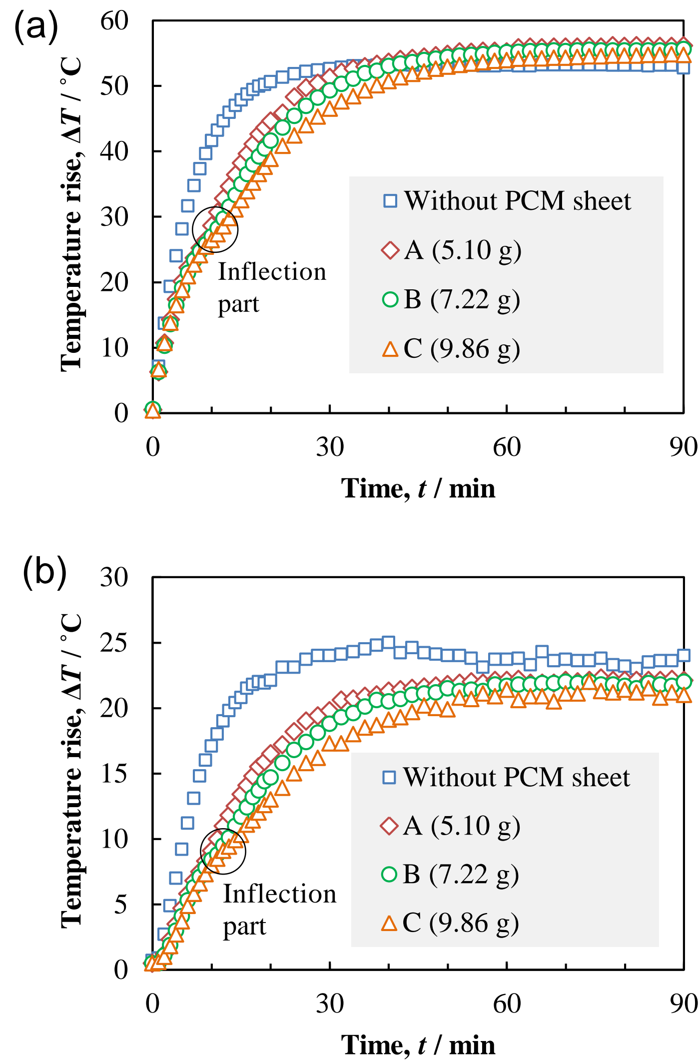

Fig. 6 Relationship between temperature rise and time. (a) Heater temperature. (b) Case temperature.

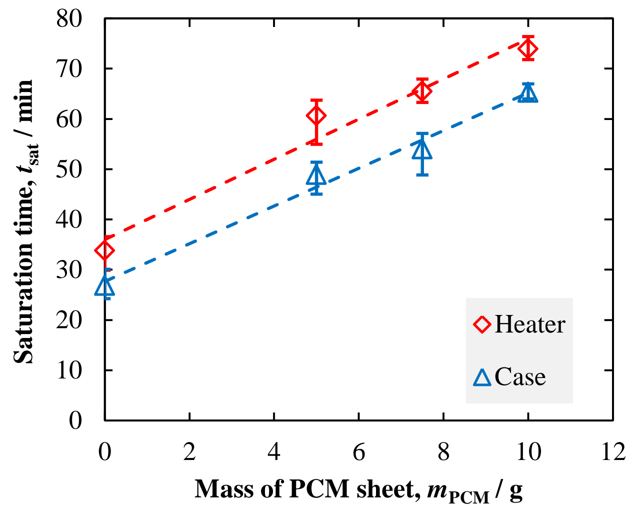

Fig. 7 Relationship between mass of PCM master batch and saturation time.

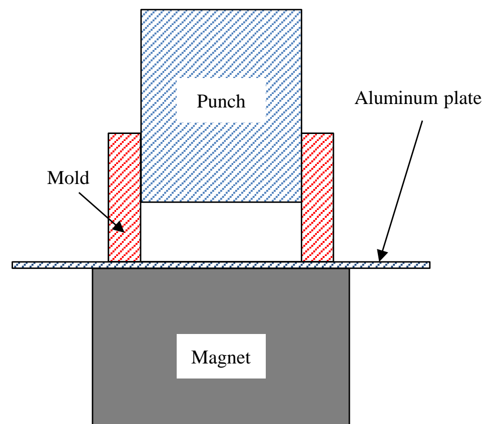

Fig. 8 Manufacturing method of modified PCM sheet.

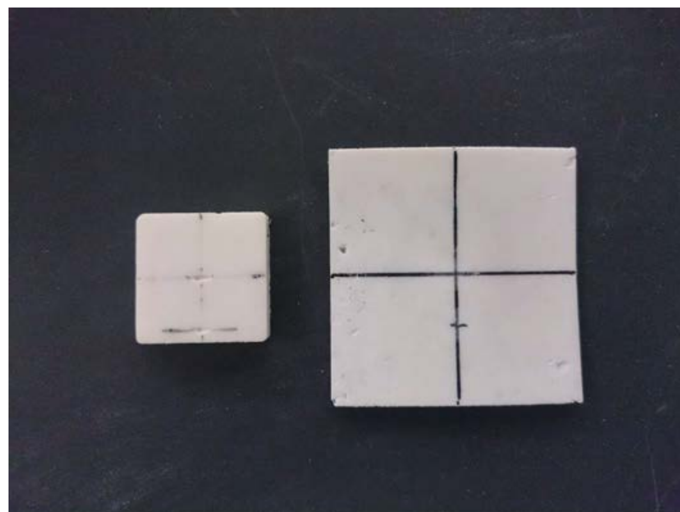

Fig. 9 Modified PCM sheet.

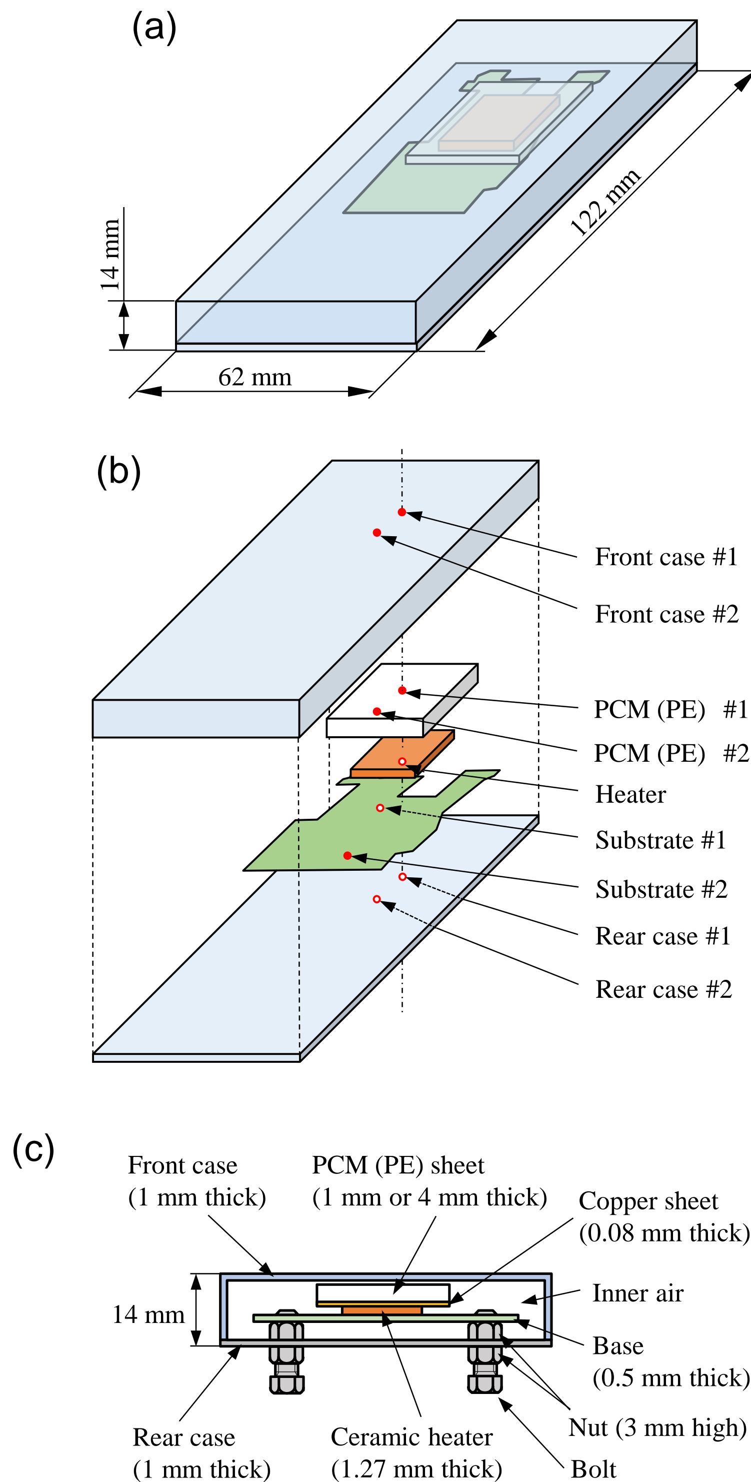

Fig. 10 Test section of the experiment on the application of the PCM sheet to the smart phone simulator. (a) Dimensions. (b) Thermocouple locations. (c) Cross-sectional view.

(a)

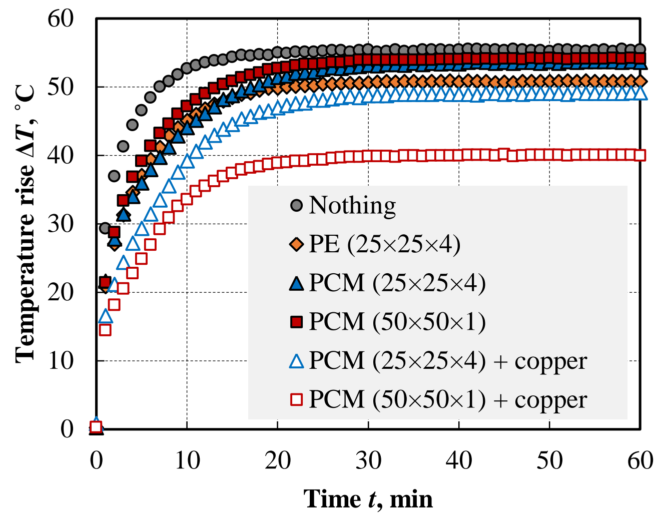

(b)

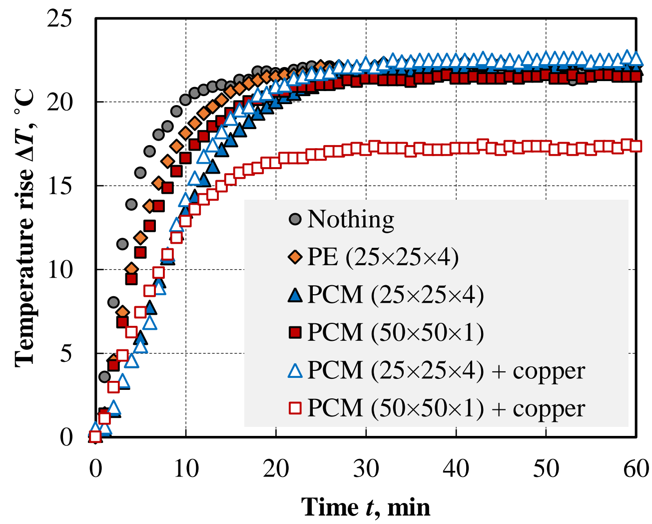

Fig. 11 Relationship between temperature rise and time. (a) Heater temperature. (b) Front case temperature.

(a)

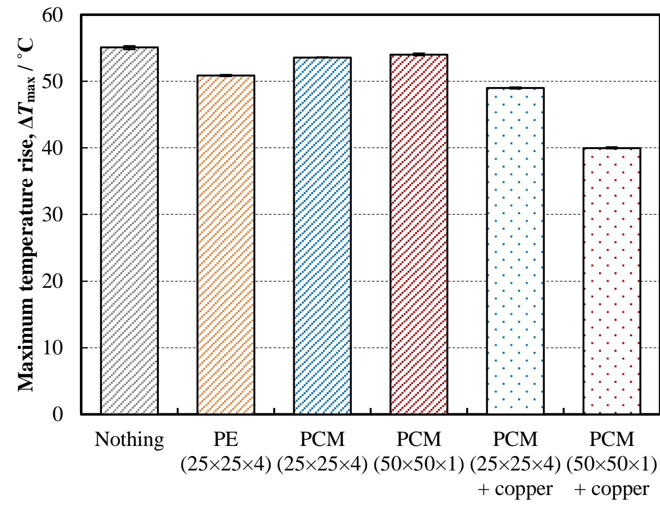

(b)

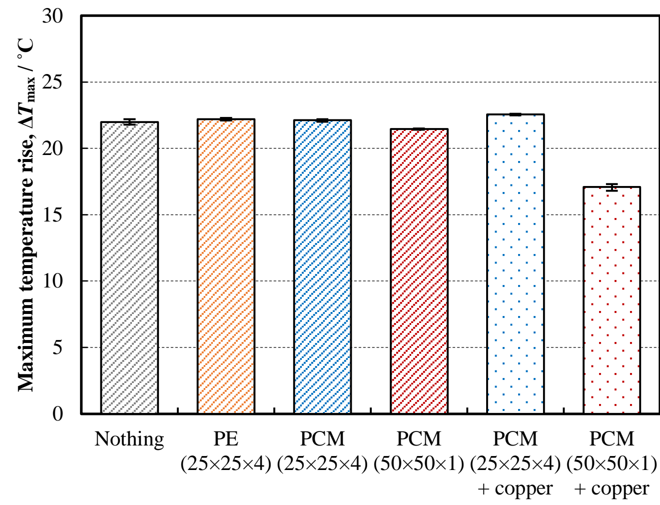

Fig. 12 Maximum temperature rise at different conditions. (a) Heater temperature. (b) Front case temperature.

(a)

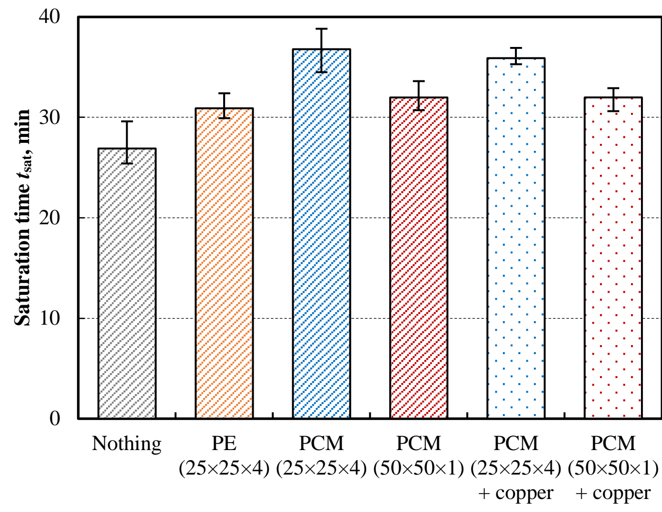

(b)

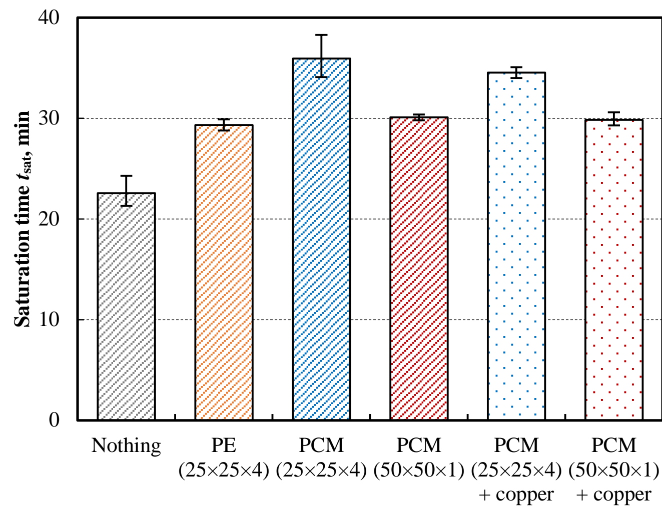

Fig. 13 Saturation time at different conditions. (a) Heater temperature. (b) Front case temperature.

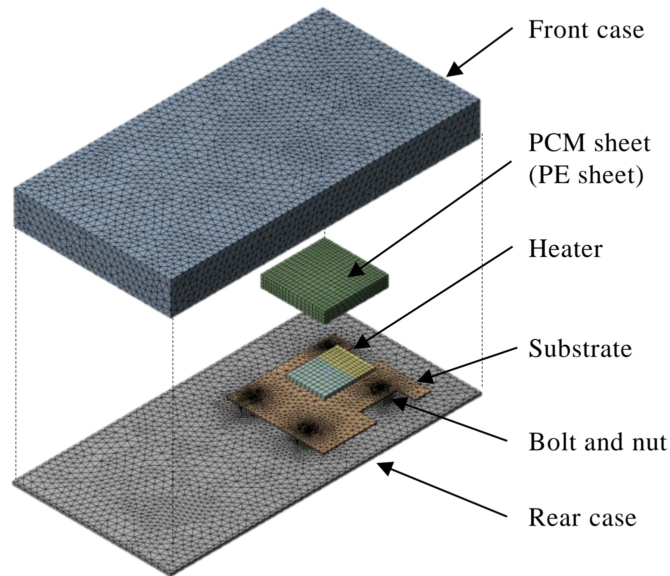

Fig. 14 Finite element model.

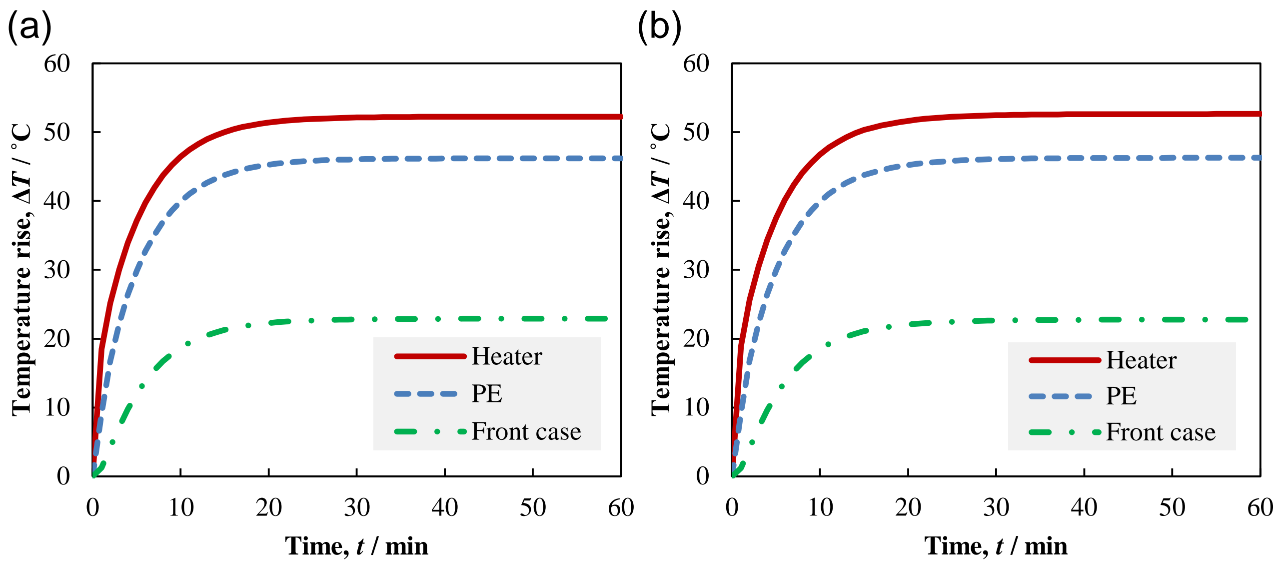

Fig. 15 Comparison between solid model and phase change model (L = 0 J/kg, μ = 1 Pa·s) with PE sheet. (a) Solid model. (b) Phase change model (L = 0 J/kg, μ = 1 Pa·s).

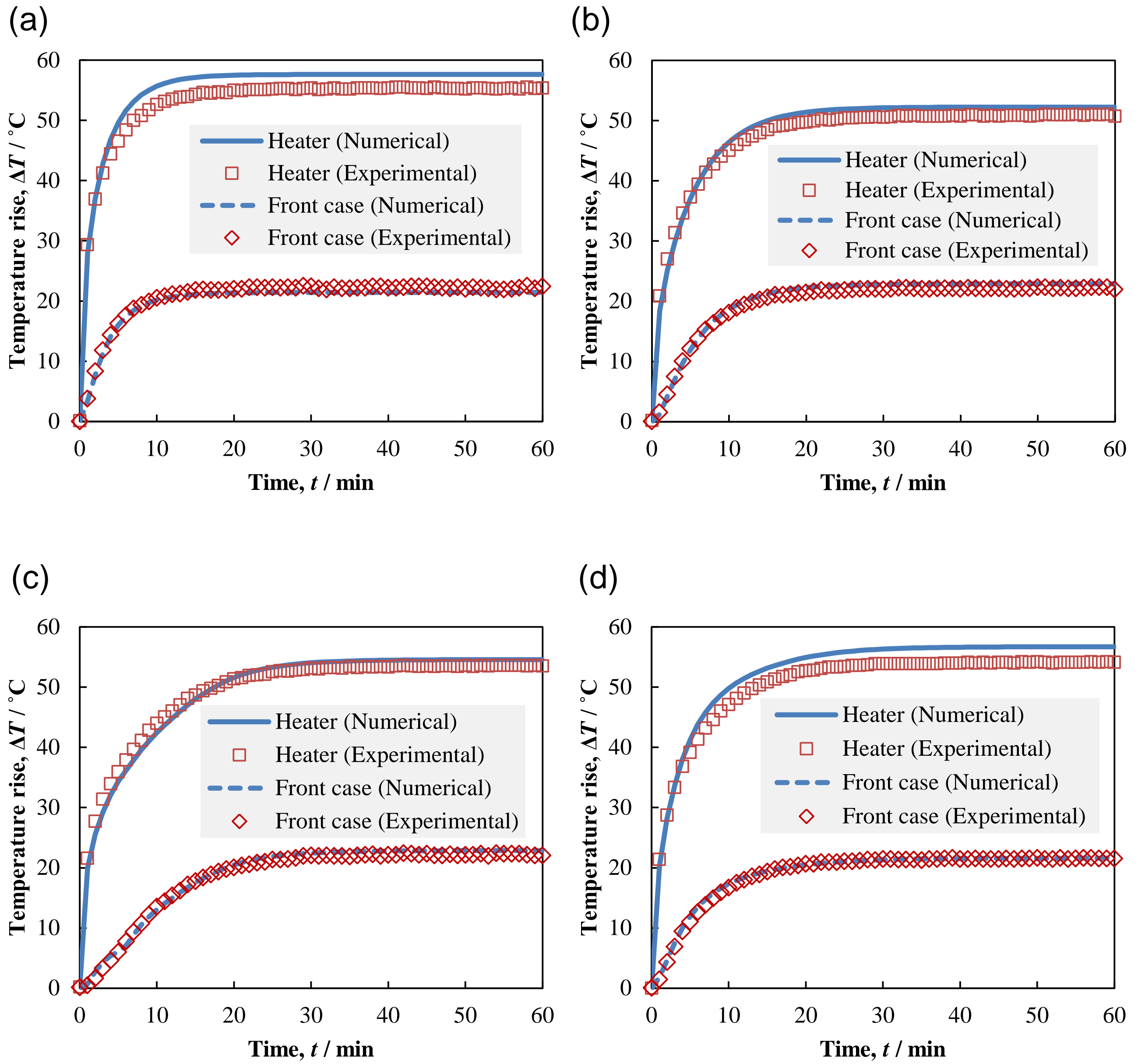

Fig. 16 Comparison between numerical results and experimental results. (a) No sheet. (b) PE sheet (25×25×4 mm). (c) PCM sheet (25×25×4 mm). (d) PCM sheet (50×50×1 mm).

Table 1 Physical properties of microencapsulated PCM.

	Melting point [°C]	Latent heat [kJ/kg]	Specific heat [kJ/kg·K]	Bulk density [kg/m^3]
PMCD-32SP	32	140-160	1.6	300-600

Table 2 Dimensions and mass of PCM sheets.

	Dimensions			Mass [g]
	Length [mm]	Width [mm]	Thickness [mm]	
PCM sheet A	100	50	1.60	5.10
PCM sheet B	100	50	2.10	7.22
PCM sheet C	100	50	2.45	9.86

Table 3 Physical properties used in the simulation.

Parts	Materials	Density [kg/m^3]	Specific heat [kJ/kg·K]	Thermal conductivity [W/m·K]	Emissivity
Front case	Polycarbonate	1200	1.20	0.19	0.9
Rear case	Acylic	1190	1.47	0.21	0.9
Substrate	Epoxy and copper	3690	0.880	25 0.5 (Thickness direction)	0.7
Heater	Ceramic	3890	0.780	18	0.7
PE sheet	Polyethylene	953	1.89	0.5	0.9
Bolt and nut	Steel	7830	0.461	16.3	0.7
Thermal tape	–	3900	0.800	0.5	–

Table 4 Estimated physical properties of PCM sheet.

Density [kg/m^3]	Specific heat [kJ/kg·K]	Thermal conductivity [W/m·K]	Emissivity
846	1.97	0.26	0.9

Latent heat [kJ/kg]	Melting temperature [°C]	Solidus temperature [°C]	Liquidus temperature [°C]
86.7	32	31	33